Received 16 May 2024; revised 12 July 2024; accepted 29 July 2024. Date of publication 5 August 2024; date of current version 4 September 2024.

Digital Object Identifier 10.1109/OJCOMS.2024.3438571

Joint Optimization of Routing, Bandwidth, and Sub-Band Allocation in Energy-Efficient THz Nano-Networks

MOHAMMED A. ALSHORBAJI [1,2] (Member, IEEE), AHMED Q. LAWEY [1] (Member, IEEE), AND SYED ALI RAZA ZAIDI [1] (Senior Member, IEEE)

[1]School of Electronic and Electrical Engineering, University of Leeds, LS2 9JT Leeds, U.K.

[2]Electrical and Electronic Engineering Department, University of Mosul, Mosul, Iraq

CORRESPONDING AUTHOR: M. A. ALSHORBAJI (e-mail: ml14maa@leeds.ac.uk)

This work was supported in part by EPSRC CHEDDAR under Grant EP/X040518/1; in part by UKRI under Grant EP/X039161/1; and in part by MSCA Horizon EU under Grant 101086218.

ABSTRACT Nano-networks are envisioned to allow several nanoscale devices to transmit and receive information. One form of such networks is electromagnetic nano-networks working within the THz band. However, high overall path loss and molecular noise experienced in the THz band, as well as limited energy storage capabilities, restrict the communication range of nano-nodes and impact network efficiency. Therefore, optimizing the nano-network resources is necessary. In this paper, we present an optimization framework employing mixed-integer linear programming (MILP) to determine the most energy-efficient routing, bandwidth, and sub-band allocation for each nano-node in an electromagnetic nano-network operating within the THz band. Our model was tested for two different scenarios related to the priority of energy saving. We also compare our proposed optimal bandwidth, routing, and sub-band allocation against less complex designs where sub-bands with fixed bandwidth are employed in nano-nodes. Furthermore, we investigate the impact of nano-node's processing and sensing units on the overall network energy consumption and the associated optimal bandwidth allocation and routing strategy. Given the considered parameters and the model's assumptions, the results show that using the optimal multi-hops paths with higher bandwidth allocation for the considered sub-bands can be more energy efficient than sending the traffic using a single hop and lower bandwidths, especially when the transmission power dominates in the nano-network. On the other hand, when the processing and sensing unit's energy consumption is dominant, then single hop schemes with lower bandwidth allocation result in the minimum network energy consumption. Finally, we discuss the limitations of the proposed energy-efficient strategies and point toward possible future research directions to which the model can be adapted.

INDEX TERMS Nano-networks, terahertz band, channel capacity, energy efficiency.

I. INTRODUCTION

NANOCOMMUNICATIONS, a cutting-edge field within the realm of nanotechnology, focuses on researching methodologies that allow the transmission of information at the nanoscale among devices and structures ranging from one to a few hundred nanometers in size. Unlike conventional communication systems, which operate at larger scales, nano-communication harnesses the unique properties of nanomaterials to enable data exchange among nano-nodes. A nano-node is the smallest component in a nano-network, and it may implement simple computational, sensing, and/or actuating tasks at the nano-level [1], [2]. A conceptual nano-node includes processing, data storage, communication, power, sensing and actuation units [3], [4], [5]. Due to their limited resources, nano-nodes need to operate cooperatively within a nano-network to perform more complex tasks and potential applications in the industry (e.g., food and fluid quality control [6]),

environment (e.g., air pollution control [7]), healthcare (e.g., drug delivery systems [8], health monitoring [9], [10]), and military applications [11].

To enable such nano-networks, several communication paradigms, including electromagnetic (EM), molecular, nanomechanical, and acoustic, have been suggested [3], [12], [13]. The authors of [14] asserted that electromagnetic (EM) and molecular communications hold significant potential in terms of the utilization of EM waves in the terahertz (THz) band and molecules as the means of communication between nano-nodes. In this work, we focus on THz band communications for nano-networks, which are also known in the literature as wireless nano-networks (WNNs) [15], [16]. Graphene-based THz nano-transceivers were proposed in [17]. However, graphene-based nano-antennas [18], [19], [20] operating in the 0.1 to 10 THz band can be incorporated into nano-nodes because their dimensions are just a few micrometers long [4] and a few tens of nanometers broad. In addition, circuitry for baseband processing, frequency conversion, filtering, and power amplification was suggested to be included in the EM transceivers in [3] to manage signals for the transmission or reception for nano-node devices.

Although the terahertz band offers extensive bandwidth, its high transmission losses [21], [22] coupled with the limited energy of nano-nodes and molecular absorption [23] severely restrict communication distances, making multi-hop routing essential [24], [25]. The authors in [24] suggested a routing framework for wireless nano-sensor networks using a hierarchical cluster-based architecture to maximize the throughput and save the average environmental energy harvested by the nano-sensors, where the nano-node adjusts its transmitting power and use single-hop or multi-hop based on the nano-sensor available energy and current load. To reduce the computational complexity of nano-nodes, an energy-efficient multi-hop routing protocol was suggested in [25], which effectively restricts the coverage area for nano-nodes and limits multi-hop forwarding. Different routing protocols for WNN are discussed in [15], [26], [27], and [28], each providing different perspectives and addressing a particular issue in the nano-network.

With an emphasis on energy efficiency, the authors in [29] optimized the joint nano-node association and resource allocation in hierarchical nano-communication networks. They provided an adaptive frequency selection and power control strategy for nano-nodes to determine the optimal frequency and transmit power. The authors in [30] developed a multi-objective optimization problem for dynamic channel allocation in THz-based nano-networks for high-resolution plant monitoring, where each nano-node adjusts its frequency based on the channel conditions to optimize the aggregated channel capacity and minimize nano-node energy consumption. Similarly, in [31], the overall network performance was optimized by introducing a frequency selection strategy for nano-devices based on the channel conditions. Different frequency selection strategies were proposed in [32] for nano-nodes in agricultural crop monitoring to respond to varying moisture levels, increase the transmission capacity, and reduce power usage. For the optimal utilization of the THz band capacity, the authors of [33] recommended simultaneous broadcasts to many nearby receivers using the optimal channel bandwidth, which can serve as the farthest receiver. They assumed that long-distance transmission utilized the centre of the higher channel bandwidth window, whereas short-distance communication used the sides without affecting long-distance receivers. However, this study did not show the effect of using different channel bandwidths on total nano-node energy consumption.

None of the above studies addressed multi-hop routing with channel adaptations. Because of the limited energy storage capability of nano-nodes [34], reducing energy consumption will always be a subject of considerable interest, which is our main objective. This is achieved through a multi-faceted strategy, by jointly optimizing traffic routing and dynamically adapting the sub-band bandwidth and allocation. This model uses Mixed Integer Linear Programming (MILP) and is solved using A Mathematical Programming Language (AMPL) software and the COIN Branch and Cut (CBC) solver.

The main contributions of this work can be summarized as follows:

- We developed a joint routing, bandwidth and sub-band allocation mathematical model using MILP to minimize the total network energy consumption for a nano-network in the THz band. To the best of our knowledge, no previous study has addressed all the three elements above jointly.
- We propose four different optimization strategies with varying adaptability, complexity, and energy efficiency levels and show at which scale each strategy is more appropriate to adopt.
- We analytically investigated the impact of adding processing/sensing units on the optimal routing, sub-bands allocated bandwidth, and total nano-network energy consumption.

The rest of this paper is organized as follows. Section II briefly explains the terahertz band channel model in terms of its propagation loss and noise. In Section III, we introduce our mathematical model. In Section IV, we present our results and analysis. Finally, we conclude the main findings in Section V.

II. TERAHERTZ BAND CHANNEL MODELLING

The authors in [21] developed a propagation model for THz EM communications over very short distances, considering the combined effects of molecule absorption noise and path losses. The total THz travelling wave path loss $A_T(f, d)$ can be written as [21]:

$$A_T(f, d) = A_{spr}(f, d) \times A_{abs}(f, d) \quad (1)$$

where f is the transmitting frequency in Hz though the distance d in meters. $A_{spr}(f, d)$ represents the spreading loss and is calculated using the free-space path loss formula [21]:

$$A_{spr}(f, d) = \left(\frac{4\pi f d}{c_0}\right)^2 \tag{2}$$

where c_0 is the speed of light in the medium. $A_{abs}(f, d)$ is the molecular absorption due to excited molecules in the medium, which absorbs a portion of the wave energy. The analytical equation for molecular absorption loss can be written as [21]:

$$A_{abs}(f, d) = \frac{1}{\tau(f, d)} = e^{K(f)\times d} \tag{3}$$

where $\tau(f, d)$ is the transmittance of the medium, $K(f)$ is the medium absorption coefficient at the frequency f. Notably, molecule absorption is a frequency-selective process. As a result, the communication distance is reduced due to the higher molecular absorption at some THz frequencies at long distances. However, the molecular absorption is negligible at transmission distances below a few tens of millimeters, where $A_{abs} \cong 1$ when $d \to 0$ [4], [22], [35], [36].

In the THz band channel, absorption by molecules in the medium not only attenuates the transmitted signal but also introduces noise. Molecular noise is the primary source of ambient noise in the THz channel [1], [37], [38]. Molecular noise is generated when molecules vibrate internally due to the incident wave and generate electromagnetic radiation at the same frequency as the propagating wave. The total noise power spectral density (P_N) can be calculated as [21]:

$$P_N(f, d) = k_B \times \left(T_{sys} + T_{mol}(f, d) + T_{other}\right) \tag{4}$$

where k_B is the Boltzmann constant, T_{mol} is the molecular noise temperature in Kelvin, T_{sys} is the system electron noise temperature, and T_{other} refers to any other additional noise source present in the medium. $T_{mol}(f, d)$ at an omnidirectional antenna can be represented as [21]:

$$T_{mol}(f, d) = T_0\left(1 - e^{-K(f)\times d}\right) \tag{5}$$

where T_0 is the reference temperature in Kelvin. When the transmission distance is short, molecular noise tends to disappear [4], [36], i.e., $T_{mol} \cong 0$ as $d \to 0$. P_N increases with an increase in the transmitting distance due to T_{mol}. Overall, by carefully selecting the center frequency, sub-bands bandwidth, and transmitting distance, we can mitigate the impact of noise and improve the signal-to-noise ratio (SNR) [30], [31], [32].

III. MILP MODEL OF ENERGY-EFFICIENCY MANO-NETWORK

In this section, a mathematical model is developed to optimize a nano-network, which is shown in Fig. 1. The model is based on the following assumptions:

- A hierarchical cluster-based architecture [24], [29], [39], [40] was considered, where the nano-sensors were responsible for collecting data from the environment. These nano-sensors typically have sensing units and basic processing units to generate digital data. Additionally, nano-relays assist in relaying data across the network toward a single nano-router, which aggregates the data and sends it to an external gateway.
- A cluster of $|N|$ nano-nodes was randomly distributed throughout the area of $(D_{max} \times D_{max})$ meters. These nano-nodes are classified as $|S|$ nano-sensors, one nano-router, and $(|N| - |S| - 1)$ nano-relays.
- Each pair of nano-nodes can communicate over a certain sub-band within the overall considered THz bandwidth.
- Each nano-node is equipped with a nano-processor, THz nano-transceiver, nano-capacitor with an energy harvesting unit, and a sensing unit for nano-sensors [3], [4], [5].
- We considered the model presented in [21] as the basis for calculating the channel capacity in our work.

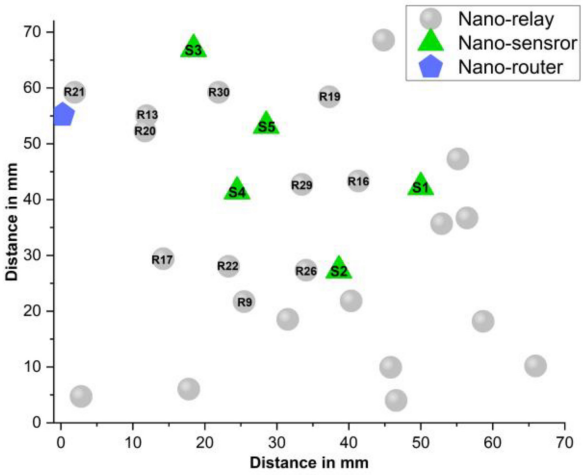

FIGURE 1. Nano-nodes placement within a cluster of *D_max* = 70 *mm*.

A. MODEL DEFINITIONS

In this section, we defined the sets, parameters, and variables before introducing the main objective function and constraints.

1) SETS

N	Set of all nano-nodes in the cluster
S	Subset of nano-sensors in the cluster
D	Subset of the nano-routers, where $\|D\| = 1$
R	Subset of nano-relays in the cluster
W	Set of the bandwidth's options available for the link between any pair of nano-nodes, $W = \{1, 2, 3 \ldots \|W\|\}$.
$\overline{\overline{F}}_w$	Set of all sub-bands configured with bandwidth option $w \in W, F_w = \{1, 2, 3 \ldots F_w\|\}$.

$\overline{F}_w$ Set of forbidden sub-bands configured with bandwidth option $w \in W$, $F_w = \{1, 2, 3 \ldots |F_w|\}$.

$F_w = \overline{\overline{F}}_w \setminus \overline{F}_w$ Set of allowed sub-bands configured with bandwidth option $w \in W, F_w = \{1, 2, 3 \ldots |F_w|\}$

2) PARAMETERS

C_o Speed of light

BZ Boltzmann constant

T_0 Reference temperature of the medium

$DM_{s,d}$ The demand between the nano-node $s \in S$ and the nano-node $d \in R$ in bits

X_n The x-axis coordinates for nano-node $n \in N$ in meters

Y_n The y-axis coordinates for nano-node $n \in N$ in meters

D_{max} The maximum cluster transmitting distance in meters

$D_{i,\ j}$ The distance between nano-node $i \in N$ *and* $j \in N$ in meters

PT Nano-nodes transmit power in Watts

PP Nano-processor processing power consumption in watts

PS_s Nano-sensor $s \in S$ sensing power consumption in watts

EC Energy storage capacity of the nano-capacitor in joule

WM Maximum allowed sub-band bandwidth in Hertz

BW_w The bandwidth of the sub-band bandwidth option $w \in W$ in Hz, where

$$BW_w = \frac{WM}{2^{(|W|-w)}} \tag{6}$$

F_{min} Minimum frequency within the considered THz range in Hertz

F_{max} Maximum frequency within the considered THz range in Hertz

$|F_w|$ Maximum number of sub-bands available for bandwidth option $w \in W$, where

$$|F_w| = \frac{(f_{max} - f_{min})}{BW_w} \tag{7}$$

$FC_{w,f}$ The center frequency of sub-band $f \in F_{w \in W}$ in Hz, where

$$FC_{wf} = f \times F_{min} + 0.5 \times \ BW_w \tag{8}$$

TS The time between consecutive pulses in seconds.

TP_w Pulse duration in seconds when the bandwidth option $w \in W$ is used, where

$$\mathrm{TP}_w = \frac{1}{\mathrm{BW}_w} \tag{9}$$

β_w Pulse duration in seconds when the bandwidth option $w \in W$ is used, where

$$\mathrm{TP}_w = \frac{1}{BW_w} \tag{10}$$

EP_w Energy per pulse in joule, where

$$EP_w = PT \times \mathrm{TP}_w \tag{11}$$

$PL_{i,j}^{w,f}$ Free space propagation loss for the link (i, j) between nano-node $i \in N$ and nano-node $j \in N$ using bandwidth option $w \in W$ and centre frequency FC_{wf}, where

$$PL_{i,j}^{w,f} = \left(\frac{4\pi \times (FC_{wf} + 0.5 \times BW_w) \times D_{ij}}{C_0}\right)^2 \tag{12}$$

$PSD_{i,j}$ Total noise power spectral density for the link (i, j) Watt/Hz, which includes the molecular absorption noise [21], [41] and system noise as an additional thermal like factor [36].

$SNR_{i,j}^{w,f}$ Received SNR in nano-node $j \in N$ for the link (i, j) at the bandwidth option $w \in W$ and sub-band $f \in F_{w \in W}$, where

$$SNR_{i,j}^{w,f} = \frac{PT}{\left(PL_{i,j}^{w,f} \times BW_w \times PSD_{i,j}\right)} \tag{13}$$

$C_{i,j}^{w,f}$ The channel capacity for the link (i, j) at the bandwidth option $w \in W$ and sub-band $f \in F_{w \in W}$ in bits/sec, where

$$C_{i,j}^{w,f} = BW_w \times \ log_2\left(1 + SNR_{i,j}^{w,f}\right) \tag{14}$$

M A large number (10^6), which is required to convert the continuous traffic variable to its binary version.

Pb The probability of sending ones

α Nano-nodes processing/sensing energy weighting parameter

$w1$ Flow weighting parameter in the objective function

$w2$ Energy consumption weighting parameter in the objective function

3) VARIABLES

In this section, we discuss the optimization variables employed in our model, as presented in Table 1.

$$ET_i = \sum_{j\ in\ N} \sum_{w\ in\ W} \sum_{f\ in\ F_w} [EP_w \times Pb + (\alpha \times TS \times (PP + PS_{i \in S}))] \times \delta_{i,j}^{w,f} \quad \forall\ i\ in\ S \cup R,\ i \neq j \tag{15}$$

$$ER_j = \sum_{i\ in\ N} \sum_{w\ in\ W} \sum_{f\ in\ F_w} [EP_w \times 0.1 + (\alpha \times TS \times PP)] \times \delta_{i,j}^{w,f} \quad \forall\ j\ in\ R \cup D,\ i \neq j \tag{16}$$

To simplify the calculation of the channel capacity parameter $C_{i,j}^{w,f}$, we make several assumptions: 1) The

TABLE 1. Model optimization variables.

Variable	Domain	Description
$\gamma_{i,j}^{s,d}$	$[0, DM_{s,d}]$	The traffic flow for the link ($i \in N, j \in N$) between nano-node $s \in S$ and nano-node $d \in D$ in bits
$\gamma b_{i,j}^{s,d}$	$\{0, 1\}$	$\gamma b_{i,j}^{s,d} = 1$ if $\gamma_{i,j}^{s,d} > 0$, $\gamma b_{i,j}^{s,d} = 0$ otherwise
$\lambda_{i,j}$	$\{0, 1\}$	$\lambda_{i,j} = 1$ if $\sum_{s\in S}\sum_{d\in D}\gamma_{i,j}^{s,d} > 0$, $\lambda_{i,j} = 0$ otherwise
$\delta_{i,j}^{w,f}$	$[0, \lvert S\rvert \times DM_{s,d}]$	The total flow through the link ($i \in N, j \in N$) using the bandwidth option $w \in W$ and the sub-band $f \in F_{w\in W}$ in bits.
$\delta b_{i,j}^{w,f}$	$\{0, 1\}$	$\delta b_{i,j}^{w,f} = 1$ if $\delta_{i,j}^{w,f} > 0$, $\delta b_{i,j}^{w,f} = 0$ otherwise
ET_i	$[0, EC]$	The energy consumption for the transmitting nano-node $i \in S \cup R$ in joule, as shown in (15).
ER_j	$[0, EC]$	The energy consumption for the receiving nano-node $j \in R \cup D$ in joule, as shown in (16), where EP_w is assumed to be 10% of the transmitting energy per pulse.

transmit power is fixed. 2) Our free space path loss calculations were intentionally overestimated by considering the highest frequency within each sub-band, ensuring that any small potential molecular absorption losses were implicitly accounted for, especially for sub-bands with high bandwidths. For sub-bands with small bandwidths, the set $|\overline{F}_w|$ is introduced to prevent the model from selecting the sub-bands where the total loss is higher than the free space loss at the highest frequency within those sub-bands. 3) The molecular absorption loss is negligible because of the short distances and specific THz range considered. 4) Molecular absorption noise that is considered for a certain sub-band and a D_{max} is the maximum molecular noise within the 0.1-1 THz band, which is the overall frequency range assumed in our model. We overestimate the molecular noise by eliminating the effect of d and f on $T_{mol}(f, d)$. This is done by calculating the maximum $T_{mol(max)}(f_{K_{max}}, d_{\max})$ at maximum D_{max} and the frequency that gives the highest $K(f)$. These assumptions will result in a slightly reduced channel capacity to ensure a linear formulation for the optimization problem.

B. MODEL CONSTRAINTS AND OBJECTIVES

The model is subject to some constraints, as shown below:

1) ROUTING CONSTRAINTS

$$\sum_{j\in N: i\neq j} \gamma_{i\ j}^{s\ d} - \sum_{j\in N: i\neq j} \gamma_{j\ i}^{s\ d} = \begin{cases} DM_{s,d} & if\ i = s \\ -DM_{s,d} & if\ i = d \\ 0 & otherwise \end{cases}$$
$$\forall s \in S,\ \forall d \in D, i \in N \tag{17}$$

Constrain (17) represents the flow conservation for the traffic flow through the nano-network.

$$\gamma_{i,j}^{s,d} \geq \gamma b_{i,j}^{s,d} \tag{18}$$
$$\gamma_{i,j}^{s,d} \leq M \times \gamma b_{i,j}^{s,d}$$
$$\forall s \in S,\ \forall d \in D, i \in N,\ j \in N : i \neq j \tag{19}$$
$$\sum_{j\in N\ :\ i\neq j} \gamma b_{i,j}^{s,d} \leq 1$$
$$\forall s \in S,\ \forall d \in D, i \in N \tag{20}$$

Constraints (18) and (19) generate a binary version of the $\gamma_{i,j}^{s,d}$, where M is a sufficiently large unitless number to ensure that $\gamma b_{i,j}^{s,d} = 1$ when $\gamma_{i,j}^{s,d}$ is greater than zero. Constrain (20) ensures that traffic splitting is prevented for each path between the source and the destination.

$$\sum_{s\in S}\sum_{d\in D} \gamma_{i,j}^{s,d} \geq \lambda_{i,j} \tag{21}$$
$$\sum_{s\in S}\sum_{d\in D} \gamma_{i,j}^{s,d} \leq M \times \lambda_{i,j}$$
$$\forall\ i \in N,\ j \in N : i \neq j \tag{22}$$

Constraints (21) and (22) generate a binary version of the total traffic flow in each link ($i \in N j \in N$), where M is a sufficiently large unitless number to ensure that $\lambda_{i,j} = 1$ when $\gamma_{i,j}^{s,d}$ is greater than zero.

$$\sum_{s\in S}\sum_{d\in D} \gamma_{i,j}^{s,d} = \sum_{w\ \in\ W} \sum_{f\ \in\ F_w} \delta_{i,j}^{w,f}$$
$$\forall i \in N,\ j \in N : i \neq j \tag{23}$$
$$\delta_{i,j}^{w,f} \geq \delta b_{i,j}^{w,f}$$
$$\forall i \in N,\ j \in N,\ w\ \in\ W,\ f \in F_w : i \neq j \tag{24}$$
$$\delta_{i,j}^{w,f} \leq M \times \delta b_{i,j}^{w,f}$$
$$\forall i \in N,\ j \in N,\ w \in W, f \in F_w : i \neq j \tag{25}$$

Constraint (23) calculates the traffic in link ($i \in N j \in N$) given that the bandwidth option $w \in W$ and sub-band $f \in F_{w\in W}$ are used for that link. Constraints (24) and (25) generate a binary version of $\delta_{i,j}^{w,f}$, where M is a sufficiently large unitless number to ensure that $\delta b_{i,j}^{w,f} = 1$ when $\delta_{i,j}^{w,f}$ is greater than zero.

2) COMMUNICATION CONSTRAINTS

$$\sum_{w\ \in\ W} \sum_{f\ \in\ F_w} \delta b_{i,j}^{w,f} \leq 1$$
$$\forall i \in N,\ j \in N : i \neq j \tag{26}$$
$$\sum_{i\ \in\ N} \sum_{j\ \in\ N\ :\ i\neq j} \delta b_{i,j}^{w,f} \leq 1$$
$$\forall\ w \in W, f \in\ F_w \tag{27}$$

Constraint (26) ensures that each link ($i \in N j \in N$) selects one bandwidth option $w \in W$ and one sub-band $f \in F_{w\in W}$. Constraint (27) avoids frequency overlapping when multiple nano-nodes use the same bandwidth option $w \in W$ to eliminate interference. These two constraints

prevent any two nodes within the same cluster from selecting the same channel bandwidth and central frequency. This approach minimizes the chance of interference by effectively managing the spectrum allocation among nodes, ensuring that overlapping frequencies do not occur within the same communication cluster.

$$\gamma_{i,j}^{s,d} = 0$$
$$\forall s \in S,\ \forall d \in D, i \in N,\ j \in N : i \neq j\ \&\ j \in S \quad (28)$$
$$\gamma_{i,j}^{s,d} = 0$$
$$\forall s \in S,\ \forall d \in D, i \in N,\ j \in N : i \neq j\ \&\ i \in D \quad (29)$$

Constraint (28) ensures that nano-sensors do not receive traffic from any other nano-node in the network. Constraint (29) ensures that the nano-router does not send traffic to any other nano-nodes in the network.

$$\frac{\lambda_{i,j}}{TS} \leq \left(\frac{C_{i,j}^{w,f} \times \delta b_{i,j}^{w,f}}{\beta_w} \right)$$
$$\forall i \in N,\ j \in N,\ w \in W, f \in F_w : i \neq j \quad (30)$$

Constraint (23) ensures that the traffic in each link does not exceed the link channel rate.

3) ENERGY CONSTRAINTS

$$(ET_i + ER_i) \leq EC$$
$$\forall\ i \in N \quad (31)$$

Constraint (31) ensures that the total energy for any nano-node does not exceed the maximum energy stored in the nano-capacitor of the nano-node.

4) OBJECTIVE FUNCTION

Finally, the objective function of the model is to minimize the weighted sum of the total flow and total network energy consumption as follows:

$$Minimise : w1 \times \left(\sum_{s \in S} \sum_{d \in D} \sum_{i \in N} \sum_{j \in N} \gamma_{i,j}^{s,d} \right) + w2 \times \left(\sum_{i \in S \cup R} ET_i + \sum_{j \in D \cup R} ER_j \right) \quad (32)$$

where $w1$ and $w2$ are used as the magnitude and unit weights to prioritise one part of the objective function over the other.

IV. RESULTS AND DISCUSSIONS

As mentioned, our model jointly optimizes the selected bandwidth option, sub-band, and routing to minimize the total energy consumption, which consists of the transmission/reception energy consumption and processing/sensing energy consumption. The parameter values used are shown in Table 2. We evaluated one nano-node cluster with different cluster areas ($1\ mm \times 1mm\ to\ 70\ mm \times 70\ mm$). This is to analyse the impact of the distance between nano-nodes on the optimal selection strategy for the sub-bands, as well as their bandwidth and routing. The total evaluated bandwidth ranges from 0.1 THz to 1 THz. The THz channel model in [21], which assumes a 10% water vapor concentration and medium temperature $T = 296\ K$, was adopted to calculate the total path loss and total noise in the THz band. $|W| = 5$ as the maximum considered sub-channel bandwidth is 100 GHz within the band of interest (0.1-1 THz) where this band is chosen because it has small molecular losses as mentioned in the paper. We selected five different bandwidth options: 100, 50, 25, 12.5, and 6.25 GHz.

We consider a scenario that does not involve a high data rate or high processing requirements, e.g., similar to the work in [5], [42]. Therefore, the spreading factor ranges from (200,000 to 12,500) depending on the assigned bandwidth option. This means that, similar to the TS-OOK, the time between pulses is much longer than the pulse duration. This is more than the typical assumed values in the literature, which are approximately 1000 [4], [35], [43]. However, this is enough to pass data of $1/TS = 500\ kbps$ which we consider in this study. Only source nano-nodes (sensors) have access to sensing units; therefore, the sensing energy consumption is not calculated for the relay and router nano-nodes. It is assumed that the symbol probabilities for logical "1" s is 1, which means that we have considered the worst-case scenario in terms of energy consumption.

The energy weighting parameter α is used to evaluate the impact of the processing/sensing energy consumption proportion on the overall optimal selection strategy. $\alpha = 0$ means that the nano-node processing/sensing energy is negligible compared to the transmitting/receiving energy, and vice versa when $\alpha > 0$. The model is sufficiently generic to be adopted in other scenarios with different assumptions or parameters. The α weight range is chosen as it covers the case of negligible processing/sensing power consumption to a value where this factor is mostly dominant compared to communication power consumption.

The D_{max} value was selected to assess the performance of the analysed approaches over a relatively wide range of distances. In addition, given the addressed node distribution, the communication fails beyond $D_{max} = 70\ mm$. $w1$ and $w2$ are chosen to balance the two factors in the optimisation function, which depends on all relevant parameters used in that function. Next, we evaluate the model under different assumptions regarding the objective function weighting parameters $w1$ and $w2$.

A. LOW PRIORITY ENERGY SAVING MODEL (LPES)

In this section, we run the model with a lower priority for the total energy consumption compared to the total network flow, that is, $w2$ uses the smallest value in its range. This case serves as a baseline to compare the energy savings obtained if a higher priority is given to energy saving, i.e., keeping the nano-node ON for longer durations before the need to recharge or go to sleep mode. We also set $\alpha = 0$ to focus on the impact of sub-band allocation and bandwidth

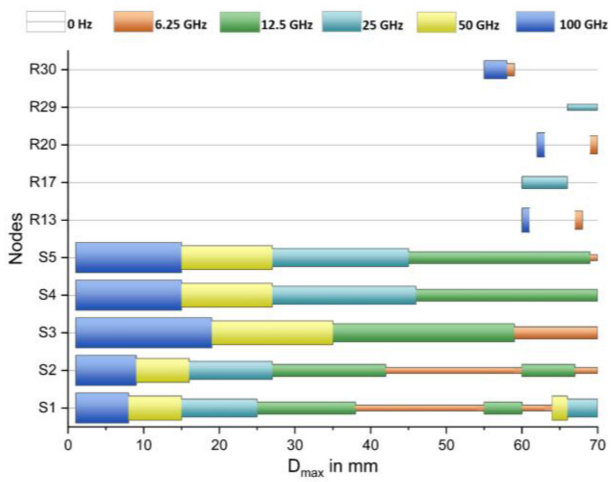

FIGURE 2. Selected bandwidth option by nano-nodes at different *D_max* using the LPES model, where $\alpha = 0$ and $PT = 1\mu W$.

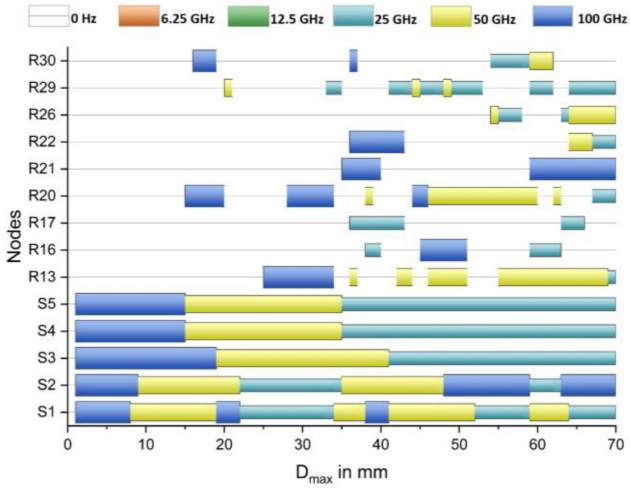

FIGURE 3. Selected bandwidth option by nano-nodes at different *D_max* using the HPES model, where $\alpha = 0$ and $PT = 1\mu W$.

strategy on transmitting/receiving energy consumption; later, we will consider higher values of α.

To explain the behaviour of LPES model, we study the optimal channel bandwidth selected by the link between each pair of turned-on nano-nodes at different D_{max}. Figure 2 shows that S1, the furthest nano-sensor from the nano-router, has selected the highest channel bandwidth of 100 GHz and uses single-hop transmission toward the destination up to D_{max} of 7 mm (i.e., when the cluster area is small ($7\ mm \times 7\ mm$). Then, a lower channel bandwidth is utilised until the point where the lowest bandwidth of 6.25 GHz is selected at D_{max} is equal to 55 mm. S1 cannot send data using a single hop through these long transmitting distances at these lower bandwidths. Therefore, the model engages R30 to turn on and works as a nano-relay for S1, i.e., switching to a multi-hop transmission, resulting in an increase in total network energy consumption. In this scenario, S1 regains its ability to utilizes a higher channel bandwidth again to save energy by decreasing TP_w. However, this will not help in reducing the overall energy consumption due to the multi-hops. Similarly, S2 used R17 to route its traffic when D_{max} increased to more than 60 mm. In contrast, S3 utilised the highest channel bandwidth, up to 18 mm rather than 7 mm, as in the S1 case, because it is the nearest node to the destination compared to all other nano-sensors.

These results show how our adaptive channel bandwidth and dynamic channel allocation framework can optimally assign a higher channel bandwidth at short transmission distances to save energy. Increasing the transmitting distance, i.e., cluster area, prompts nano-nodes to select a lower bandwidth channel until a certain point where the lowest bandwidth channel cannot be achieved because the channel rate is less than the required data rate; at this point, the traffic will be forwarded to its destination via a nano-relay. The use of multi-hop rather than single-hop when increasing the cluster area further supports the observation that due to the high spreading loss and absorption noise, the maximum transmission range is severely constrained inside the THz band [1], [53].

B. HIGHER PRIORITY ENERGY SAVING MODEL (HPES)

In this section, we run the model with a higher priority for total energy consumption compared to the total network flow, i.e., $w2$ uses the largest value in its range. Similar to the LPES model, we set $\alpha = 0$.

Figure 3 reveals that the HPES model tunes on a larger number of nano-relays across most of the considered cluster areas compared to LPES. This strategy reduces the distance between pairs of communicating nano-nodes. The smaller distances enable the nano-nodes to operate at higher bandwidths and, hence, at the shortest possible pulse duration *TP_w* which minimizes the overall energy consumption in transmitting/receiving bits at levels not attainable by LPES.

Figure 3 clearly illustrates that no channel bandwidth less than 25 GHz is selected using the HPES model compared with the LPES model, which utilizes lower channel bandwidth and hence a longer *TP_w*. For example, S1 has used several nano-relays at different cluster areas, e.g., R20 when $D_{max} = 15\ mm$, and R29, R13, and R21 when $D_{max} = 70\ mm$. The optimal routing strategy for S1 in two different cluster areas is shown in Fig. 4.

Regarding sub-band allocation, both the LPES and HPES models select the available sub-band that has the lowest central frequency to achieve the required data rate (refer to (12), (13), and (14)). This selection aims to use the highest available sub-band bandwidth option to minimize the total network energy consumption. In summary, when processing/sensing energy is not dominant, using nano-relays is more energy efficient than sending directly when the maximum cluster transmitting distance $D_{max} \geq 15$mm (given the parameters used) to minimize the high propagation

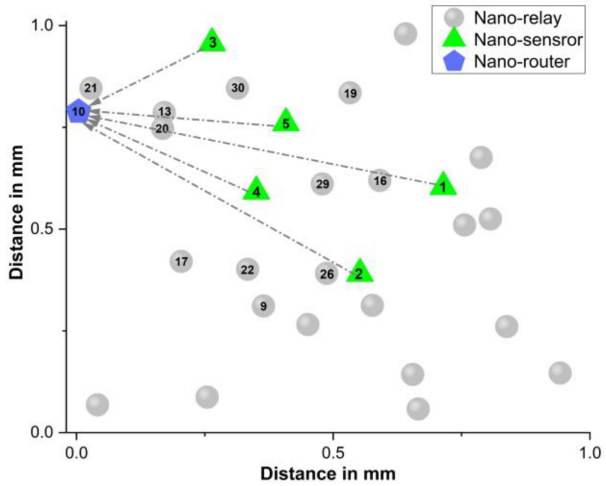

(a) Cluster area $1\ mm \times 1\ mm$

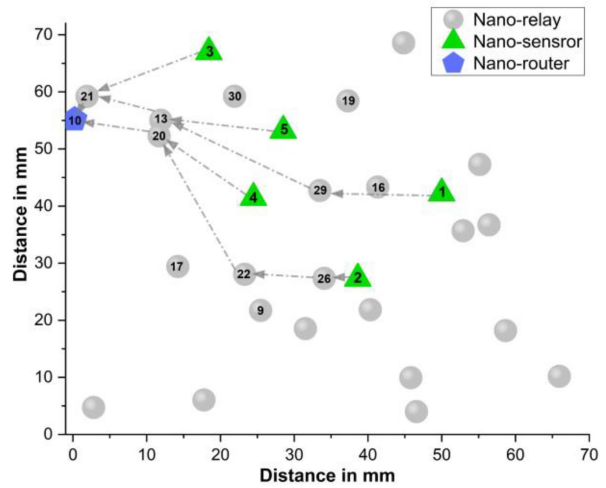

(b) Cluster area $70\ mm \times 70\ mm$

FIGURE 4. Network traffic flow at short and long transmitting distances using the HPES model.

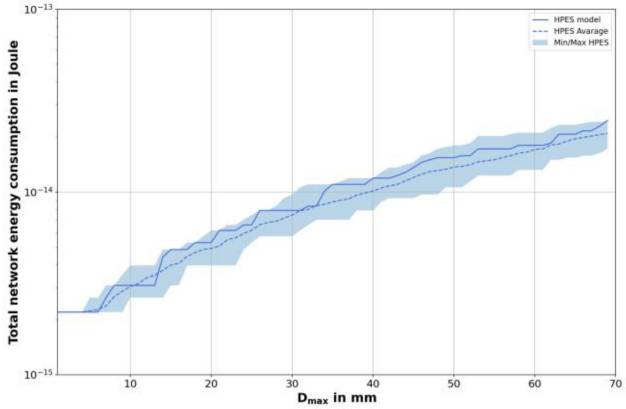

FIGURE 5. A comparison of the total network energy consumption for the HPES model between the node distribution case considered in the previous sections versus 25 different node location distributions, where $\alpha = 0$ and $PT = 1\mu W$

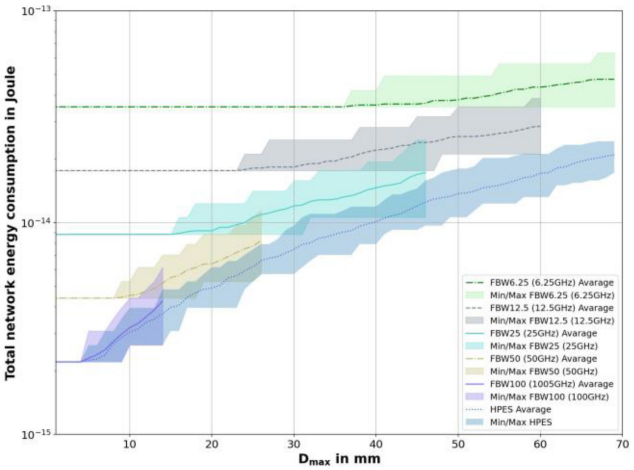

FIGURE 6. A comparison of the total network energy consumption between five different fixed bandwidth channels and our HPES model using 30 nano-nodes with 25 different node location distributions, where $\alpha = 0$ and $PT = 1\mu W$.

losses and molecular absorption noise at large distances, as explained in Section II.

In Figure 5, we test the performance of the HPES under 25 different node location distributions at different D_{max} values and with α=0 and compare its energy consumption with the node distribution case considered in the previous sections. The results show that the total energy consumption of the node distribution case considered in the previous sections does not deviate by a high margin from the average results for different node location distributions.

C. HPES FIXED VS ADAPTIVE SUB-BAND BANDWIDTHS

The requirement that nano-nodes have the ability to adapt their selected sub-band bandwidth in HPES to save energy consumption imposes a higher level of complexity in the design of nano-nodes, where their limited size might pose a challenge. In this section, we compare the performance of HPES to a simpler design approach in which each nano-node is configured with a pre-determined fixed sub-band bandwidth option [29]. This value was evaluated again at $\alpha = 0$.

Figure 6 shows that the average total energy consumption for the HPES is lower than that of the other approaches considered. In addition, selecting a higher fixed bandwidth option, (e.g., 100 GHz), would consume less energy than a smaller fixed bandwidth option, but it can only be used for short distances, up to $D_{max} = 14$ mm using the parameters in Table 2. When the D_{max} increases, selecting a higher bandwidth is not optimal because the achieved channel rate is less than the required data rate. Therefore, lower fixed channel bandwidths should be used at longer distances, with the price of consuming more energy due to the longer pulse duration. These results hint toward a new optimization problem in which the objective is to optimally match the

TABLE 2. Units for magnetic properties.

Symbol	Value and Unit
PT	1 µW [5], [36], [44], [45], [46], [47], [48].
PP	140 nW [42], including RAM and ROM memory power consumption.
PS	50 nW [42]
TS	2 µsec [5], [42]
EC	800 pJ [49]
D_{max}	From 1 mm to 70 mm
$\|W\|$	5
WM	0.1 THz [50]
F_{min}	0.1 THz [21], [50]
F_{max}	1 THz [42], [5], [51]
$\bar{F}_w$	$\bar{F}_{12.5} = \{556.25, 768.75, 968.75\}\ in\ GHz$ $\bar{F}_{6.25} = \{553.125, 765.625, 971.875\}\ in\ GHz$
Pb	1 (worst-case scenario) [52]
BZ	1.38×10^{-23} J/K
T_o	296 K [21]
C_o	2.9979×10^8 m/s
$DM_{s,d}$	40 bits (5 bytes) [42]
α	$0 < \alpha < 1 \times 10^{-3}$
$w1$	$1 < w1 < 100$
$w2$	$10^{10} < w2 < 10^{20}$

sub-set of nano-nodes with fixed sub-band allocation and bandwidth to enable end-to-end communication within the nano-network.

D. THE IMPACT OF PROCESSING AND SENSING UNITS

In this section, we compare the LPES and HPES models against the following two fixed sub-band bandwidth approaches: Fixed BW of 100 GHz (FBW100) and Fixed BW of 6.25 GHz (FBW6.25). We consider two scenarios, each with a different value of α ($\alpha = 0.01 \times 10^{-3}$, *and* $\alpha = 1 \times 10^{-3}$) to investigate the impact of adding processing/sensing units on the overall network energy consumption.

Figure 7(a) shows the results when $\alpha = 0.01 \times 10^{-3}$. We observe that the FBW6.25 model consumes more energy than the other three models because it utilises the longest pulse duration. This is even though FBW6.25 uses a minimal number of hops overall. On the other hand, FBW100 saves energy compared with the FBW6.25 model due of the shorter pulse durations. However, as the D_{max} increases, the average total network energy consumption for the FBW100 model increases significantly because of the use of multi-hop rather than single-hop, which leads to an increase in the average total energy consumption. Moreover, the FBW100 model is unable to serve the nano-sensors when the $D_{max} \geq 14$ *mm* due to the higher propagation losses, which violate constraint (19). The only possible solution is to increase the nano-relay density to minimize the distance between them.

The HPES and LPES models show better overall performance; they have almost similar average total energy consumption at smaller D_{max} values, as they follow almost

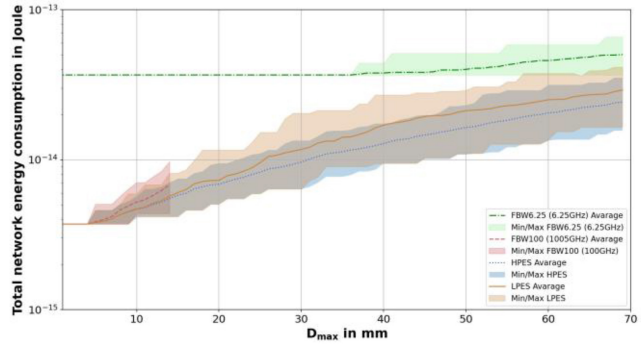

(a) $\alpha = 0.01 \times 10^{-3}$

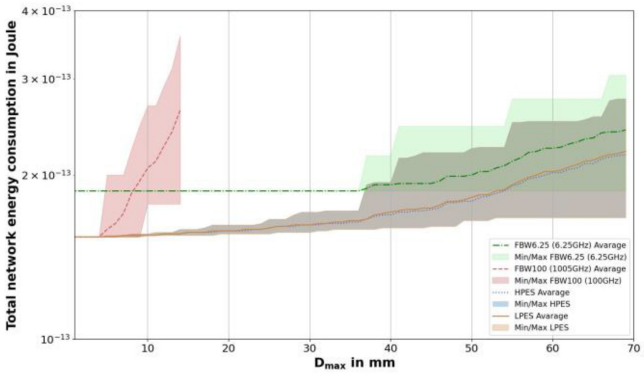

(b) $\alpha = 1 \times 10^{-3}$

FIGURE 7. A comparison of the total network energy consumption at different *D_max* between our LPES and HPES models with the FBW100 and FBW100 models with 25 different node location distributions; when $PT = 1\mu W$ and (a) $\alpha = 0.01 \times 10^{-3}$, and (b) $\alpha = 1 \times 10^{-3}$.

similar bandwidth and sub-band allocations, i.e., a single hop with a large bandwidth option. At higher values of D_{max}, we note again that HPES consumes lower average total energy than LPES, because it uses a higher number of hops with a larger bandwidth option than LPES. This saving occurs despite the fact that more processing units are used in the nano-relays because of the small value of α. For example, when $D_{max} = 70$ *mm*, the HPES model starts to turn on six nano-relays and utilizes higher bandwidth options, whereas the LPES model uses only two nano-relays with smaller bandwidth options. Overall, and given the parameters in our model, HPES can save energy up to 26% compared to LPES when $D_{max} = 42$ *mm*, and up to 19% at $D_{max} = 14$ *mm* compared to FBW100, and definitely even higher savings compared to FBW6.25.

In the second scenario ($\alpha = 1 \times 10^{-3}$), the nano-node processing/sensing energy is not negligible, whereas multi-hops are costly in terms of energy consumption. Therefore, as shown in Fig. 7(b), the average total network energy consumption for the HPES and LPES models are almost identical, because both use single hops with lower bandwidth options to minimize the energy consumption induced by multi-hops. However, both the HPES and LPES models

still saved energy compared with the FBW6.25 model, where this energy saving decreased from 17.6% to 10% by increasing *D_max* from 1 mm to 70 mm, respectively. This implies that at a higher D_{max}, using FBW6.25 is almost optimal. Finally, the average total network energy consumption for the FBW100 model is almost optimal at smaller D_{max} values, and it is the highest energy-consuming approach at higher D_{max} values because of the use of multi-hops, which consume significant energy in nano-relay processing units.

Finally, we discuss some limitations of our study. The nano-router should be part of a larger-scale system with access to sufficient energy and processing power to implement the model or heuristic version. The parameters and optimal variables must be exchanged between the nano-router and the other nano-nodes. This can be achieved by dedicating one specific sub-band to this purpose or using lower layer simple pulse-based communication, e.g., TS-OOK. As mentioned before, the fact that we require nano-nodes to adapt to sub-band allocation and bandwidth may be challenged by the small size of those nodes. One remedy is to push the complexity to fewer nano-relays and connect the nano-sensors to those relays using other communication methods, e.g., pulse, pulse-based TS-OOK using the full THz band or molecular communications. The channel capacity model from [21], which we used as the basis to calculating the channel capacity for the links between nano-nodes, is an upper bound, which means that any further noise present in the system will reduce the overall communication distance. Similarly, higher water vapor concentrations also limit the communication distance, i.e., the range of D_{max} values will be lower than what we have considered in this work, and the impact of such cases on routing, bandwidth and sub-band allocation warrants further investigation. Our current model does not incorporate blocking effects, where terahertz waves are highly sensitive to physical obstructions [54]. Although we are aware of these challenging aspects and assumptions of the envisioned nano-nodes, we hope that providing such a mathematical framework will contribute to a better understanding of the impact of such assumptions on the overall performance of nano-networks.

V. CONCLUSION

This paper introduces a MILP model to study the joint optimization of the sub-band bandwidth and dynamic channel allocation to minimize the energy consumption of electromagnetic nano-networks in the THz band. We compared four different strategies, one of which was the most optimal strategy at all nano-network scales, whereas the other three work differently at different nano-network scales. Our results show that with a fixed number of nano-nodes and a smaller network area, using sub-bands with a large bandwidth is almost optimal, and vice versa for larger network areas. This trend is mostly noticeable when we include the extra energy consumption due to processing and sensing units in the nano-nodes. Using the optimal number of multi-hops with higher sub-band bandwidths can be more energy efficient than sending traffic using a single hop and lower bandwidth, especially when the transmission power dominates in the nano-network. Moreover, the model is flexible enough to account for other scenarios that we did not consider in this work, e.g., hybrid and multi-band nano-networks, which will be addressed in our future work. In addition, we aim to extend our model to simulate a more complex environment, e.g., intra-body nano communication, to address challenges such as signal attenuation, further noise sources, and dynamic changes within such environments. This will enable the exploration of potential applications in areas such as targeted drug delivery and bio-sensing. Additionally, we plan to incorporate the movement of nano-nodes into our model, moving beyond the limitations of a static topology. This will provide a more realistic representation of nano-networks and allow the investigation of dynamic routing protocols. Furthermore, we will integrate node/link failure and its impact on blocking, e.g., due to the obstruction of signal propagation by obstacles within the environment, leading to improved simulation accuracy. To enhance the efficiency and adaptability of the model, we will explore the development of a heuristic version or the implementation of reinforcement learning techniques. We believe that these advancements will pave the way for a comprehensive and versatile simulation tool for nano-communication networks.

REFERENCES

[1] I. F. Akyildiz, J. M. Jornet, and C. Han, "Terahertz band: Next frontier for wireless communications," *Phys. Commun.*, vol. 12, pp. 16–32, Sep. 2014.

[2] A. Nayyar, V. Puri, and D.-N. Le, "Internet of Nano Things (IoNT): Next evolutionary step in nanotechnology," *Nanosci. Nanotechnol.*, vol. 7, no. 1, pp. 4–8, 2017.

[3] I. F. Akyildiz and J. M. Jornet, "Electromagnetic wireless nanosensor networks," *Nano Commun. Netw.*, vol. 1, no. 1, pp. 3–19, Mar. 2010.

[4] J. Josep Miquel and F. A. Ian, *Fundamentals of Electromagnetic Nanonetworks in the Terahertz Band*. Hanover, MA, USA: Now Publ., 2013.

[5] S. Canovas-Carrasco, A.-J. Garcia-Sanchez, F. Garcia-Sanchez, and J. Garcia-Haro, "Conceptual design of a nano-networking device," *Sensors*, vol. 16, no. 12, p. 2104, 2016.

[6] J. W. Aylott, "Optical nanosensors–an enabling technology for intracellular measurements," *Analyst*, vol. 128, no. 4, pp. 309–312, 2003.

[7] J. Han, J. Fu, and R. B. Schoch, "Molecular sieving using nanofilters: Past, present and future," *Lab Chip*, vol. 8, no. 1, pp. 23–33, 2008.

[8] R. A. Freitas, Jr., "Pharmacytes: An ideal vehicle for targeted drug delivery," *J. Nanosci. Nanotechnol.*, vol. 6, nos. 9–10, pp. 2769–2775, Oct. 2006.

[9] M. Witt and W. Wozniak, "Structure and function of the vomeronasal organ," *Adv. Otorhinolaryngol*, vol. 63, pp. 70–83, 2006.

[10] B. Atakan, O. B. Akan, and S. Balasubramaniam, "Body area nanonetworks with molecular communications in nanomedicine," *IEEE Commun. Mag.*, vol. 50, no. 1, pp. 28–34, Jan. 2012.

[11] R. E. Smalley, *Carbon Nanotubes: Synthesis, Structure, Properties, and Applications*. Berlin, Germany: Springer, 2003.

[12] N. Agoulmine, K. Kim, S. Kim, T. Rim, J. Lee, and M. Meyyappan, "Enabling communication and cooperation in bio-nanosensor networks: Toward innovative healthcare solutions," *IEEE Wireless Commun.*, vol. 19, no. 5, pp. 42–51, Oct. 2012.

[13] J. R. Vacca, *Nanoscale Networking and Communications Handbook*. Boca Raton, FL, USA: CRC Press, 2019.

[14] I. F. Akyildiz, F. Brunetti, and C. Blázquez, "Nanonetworks: A new communication paradigm," *Comput. Netw.*, vol. 52, no. 12, pp. 2260–2279, 2008.

[15] X.-W. Yao, Y.-C.-G. Wu, and W. Huang, "Routing techniques in wireless nanonetworks: A survey," *Nano Commun. Netw.*, vol. 21, Sep. 2019, Art. no. 100250.

[16] L. Aliouat, M. Rahmani, H. Mabed, and J. Bourgeois, "Enhancement and performance analysis of channel access mechanisms in Terahertz band," *Nano Commun. Netw.*, vol. 29, Sep. 2021, Art. no. 100364.

[17] J. M. Jornet and I. F. Akyildiz, "Graphene-based plasmonic nano-transceiver for Terahertz band communication," in *Proc. 8th Eur. Conf. Antennas Propag. (EuCAP 2014)*, 2014, pp. 492–496.

[18] J. M. Jornet and I. F. Akyildiz, "Graphene-based nano-antennas for electromagnetic nanocommunications in the Terahertz band," in *Proc. 4th Eur. Conf. Antennas Propag.*, 2010, pp. 1–5.

[19] J. M. Jornet and I. F. Akyildiz, "Graphene-based plasmonic nano-antenna for Terahertz band communication in nanonetworks," *IEEE J. Sel. Areas Commun.*, vol. 31, no. 12, pp. 685–694, Dec. 2013.

[20] M. Tamagnone, J. S. Gómez-Díaz, J. R. Mosig, and J. Perruisseau-Carrier, "Reconfigurable Terahertz plasmonic antenna concept using a graphene stack," *Appl. Phys. Lett.*, vol. 101, no. 21, 2012, Art. no. 214102.

[21] J. M. Jornet and I. F. Akyildiz, "Channel modeling and capacity analysis for electromagnetic wireless nanonetworks in the Terahertz band," *IEEE Trans. Wireless Commun.*, vol. 10, no. 10, pp. 3211–3221, Oct. 2011.

[22] J. M. Jornet and I. F. Akyildiz, "Channel capacity of electromagnetic nanonetworks in the Terahertz band," in *Proc. IEEE Int. Conf. Commun.*, 2010, pp. 1–6.

[23] I. T. Javed and I. H. Naqvi, "Frequency band selection and channel modeling for WNSN applications using simplenano," in *Proc. IEEE Int. Conf. Commun. (ICC)*, 2013, pp. 5732–5736.

[24] M. Pierobon, J. M. Jornet, N. Akkari, S. Almasri, and I. F. Akyildiz, "A routing framework for energy harvesting wireless nanosensor networks in the Terahertz band," *Wireless Netw.*, vol. 20, no. 5, pp. 1169–1183, Jul. 2014.

[25] J. Xu, R. Zhang, and Z. Wang, "An energy efficient multi-hop routing protocol for Terahertz wireless nanosensor networks," in *Proc. Int. Conf. Wireless Algorithms, Syst., Appl.*, 2016, pp. 367–376.

[26] A. O. Balghusoon and S. Mahfoudh, "Routing protocols for wireless nanosensor networks and Internet of Nano Things: A comprehensive survey," *IEEE Access*, vol. 8, pp. 200724–200748, 2020.

[27] F. Lemic et al., "Survey on Terahertz nanocommunication and networking: A top-down perspective," 2019, *arXiv:1909.05703*.

[28] N. Saeed, M. H. Loukil, H. Sarieddeen, T. Y. Al-Naffouri, and M. S. Alouini, "Body-centric Terahertz networks: Prospects and challenges," *IEEE Trans. Mol., Biol. Multi-Scale Commun.*, vol. 8, no. 3, pp. 138–157, Sep. 2022.

[29] L. Feng, Q. Yang, D. Park, and K. S. Kwak, "Energy efficient nano-node association and resource allocation for hierarchical nano-communication networks," *IEEE Trans. Mol., Biol. Multi-Scale Commun.*, vol. 4, no. 4, pp. 208–220, Dec. 2018.

[30] A. Afsharinejad, A. Davy, and B. Jennings, "Dynamic channel allocation in electromagnetic nanonetworks for high resolution monitoring of plants," *Nano Commun. Netw.*, vol. 7, pp. 2–16, Mar. 2016.

[31] A. Afsharinejad, A. Davy, B. Jennings, and S. Balasubramaniam, "GA-based frequency selection strategies for graphene-based nano-communication networks," in *Proc. IEEE Int. Conf. Commun. (ICC)*, 2014, pp. 3642–3647.

[32] A. Afsharinejad, A. Davy, and B. Jennings, "Frequency selection strategies under varying moisture levels in wireless nano-networks," presented at the Proc. ACM 1st Annu. Int. Conf. Nanoscale Comput. Commun., Atlanta, GA, USA, 2014.

[33] C. Han and I. F. Akyildiz, "Distance-aware multi-carrier (DAMC) modulation in Terahertz band communication," in *Proc. IEEE Int. Conf. Commun. (ICC)*, 2014, pp. 5461–5467.

[34] Z. L. Wang, "Towards self-powered nanosystems: From nanogenerators to nanopiezotronics," *Adv. Funct. Mater.*, vol. 18, no. 22, pp. 3553–3567, 2008.

[35] J. M. Jornet and I. F. Akyildiz, "Information capacity of pulse-based wireless nanosensor networks," in *Proc. 8th Annu. IEEE Commun. Soc. Conf. Sensor, Mesh Ad Hoc Commun. Netw.*, 2011, pp. 80–88.

[36] I. Llatser et al., "Scalability of the channel capacity in graphene-enabled wireless communications to the nanoscale," *IEEE Trans. Commun.*, vol. 63, no. 1, pp. 324–333, Jan. 2015.

[37] P. Boronin, D. Moltchanov, and Y. Koucheryavy, "A molecular noise model for THz channels," in *Proc. IEEE Int. Conf. Commun. (ICC)*, 2015, pp. 1286–1291.

[38] J. M. Jornet and I. F. Akyildiz, "Femtosecond-long pulse-based modulation for Terahertz band communication in nanonetworks," *IEEE Trans. Commun.*, vol. 62, no. 5, pp. 1742–1754, May 2014.

[39] S. Tairin, N. Nurain, and A. A. Al Islam, "Network-level performance enhancement in wireless nanosensor networks through multi-layer modifications," in *Proc. Int. Conf. Netw., Syst. Secur. (NSysS)*, 2017, pp. 75–83.

[40] G. Piro, L. A. Grieco, G. Boggia, and P. Camarda, "Nano-Sim: Simulating electromagnetic-based nanonetworks in the network simulator 3," in *Proc. SimuTools*, 2013, pp. 203–210.

[41] S. Paine. "The am atmospheric model." 2019. [Online]. Available: https://zenodo.org/records/1193771

[42] S. Canovas-Carrasco, A.-J. Garcia-Sanchez, and J. Garcia-Haro, "A nanoscale communication network scheme and energy model for a human hand scenario," *Nano Communi. Netw.*, vol. 15, pp. 17–27, Mar. 2018.

[43] R. G. Cid-Fuentes, J. M. Jornet, I. F. Akyildiz, and E. Alarcón, "A receiver architecture for pulse-based electromagnetic nanonetworks in the Terahertz Band," in *Proc. IEEE Int. Conf. Commun. (ICC)*, 2012, pp. 4937–4942.

[44] P. M. Shree, T. Panigrahi, and M. Hassan, "Classifying the order of higher derivative gaussian pulses in Terahertz wireless communications," in *Proc. IEEE Globecom Workshops (GC Wkshps)*, 2018, pp. 1–6.

[45] G. Piro, P. Bia, G. Boggia, D. Caratelli, L. A. Grieco, and L. Mescia, "Terahertz electromagnetic field propagation in human tissues: A study on communication capabilities," *Nano Commun. Netw.*, vol. 10, pp. 51–59, Dec. 2016.

[46] F. Afsana, M. Asif-Ur-Rahman, M. R. Ahmed, M. Mahmud, and M. S. Kaiser, "An energy conserving routing scheme for wireless body sensor nanonetwork communication," *IEEE Access*, vol. 6, pp. 9186–9200, 2018.

[47] F. S. Lee and A. P. Chandrakasan, "A 2.5 nJ/bit 0.65 V pulsed UWB receiver in 90 nm CMOS," *IEEE J. Solid-State Circuits*, vol. 42, no. 12, pp. 2851–2859, Dec. 2007.

[48] Q. H. Abbasi, A. A. Nasir, K. Yang, K. A. Qaraqe, and A. Alomainy, "Cooperative in-vivo nano-network communication at Terahertz frequencies," *IEEE Access*, vol. 5, pp. 8642–8647, 2017.

[49] J. M. Jornet, "A joint energy harvesting and consumption model for self-powered nano-devices in nanonetworks," in *Proc. IEEE Int. Conf. Commun. (ICC)*, 2012, pp. 6151–6156.

[50] P. Boronin, V. Petrov, D. Moltchanov, Y. Koucheryavy, and J. M. Jornet, "Capacity and throughput analysis of nanoscale machine communication through transparency windows in the Terahertz band," *Nano Commun. Netw.*, vol. 5, no. 3, pp. 72–82, Sep. 2014.

[51] T. Kleine-Ostmann, C. Jastrow, S. Priebe, M. Jacob, T. Kürner, and T. Schrader, "Measurement of channel and propagation properties at 300 GHz," in *Proc. Conf. Precision Electromag. Meas.*, 2012, pp. 258–259.

[52] S. Canovas-Carrasco, R. Asorey-Cacheda, A. J. Garcia-Sanchez, J. Garcia-Haro, K. Wojcik, and P. Kulakowski, "Understanding the applicability of Terahertz flow-guided nano-networks for medical applications," *IEEE Access*, vol. 8, pp. 214224–214239, 2020.

[53] H. Yu, B. Ng, and W. K. G. Seah, "Forwarding schemes for EM-based wireless nanosensor networks in the Terahertz band," presented at the Proc. 2nd Annu. Int. Conf. Nanoscale Comput. Commun., Boston, MA, USA, 2015.

[54] S. Ghafoor, N. Boujnah, M. H. Rehmani, and A. Davy, "MAC protocols for Terahertz communication: A comprehensive survey," *IEEE Commun. Surveys Tuts.*, vol. 22, no. 4, pp. 2236–2282, 4th Quart., 2020.

MOHAMMED A. ALSHORBAJI (Member, IEEE) received the B.Sc. degree (Hons.) in electrical engineering/electronics and communication from Mosul University, Mosul, Iraq, in 2009, and the M.Sc. degree (Hons.) in electronic and electrical engineering from the University of Leeds, U.K., in 2016, where he is currently pursuing the Ph.D. degree in electrical engineering. He has been a Lecturer with the College of Engineering, Mosul University since 2010. His research interests lie in the areas of nanonetworks, Internet of Nano Things, network energy efficiency, and terahertz band communication.

AHMED Q. LAWEY (Member, IEEE) received the B.S. and M.Sc. degrees (Hons.) in computer engineering from the University of Al-Nahrain, Iraq, in 2002 and 2005, respectively, and the Ph.D. degree in communication networks from the University of Leeds, U.K., in 2015.

From 2005 to 2010, he was a Core Network Engineer with ZTE Corporation for Telecommunication, Iraq. He is currently a Lecturer of Communication Networks with the School of Electronic and Electrical Engineering, University of Leeds. His current research interests include energy efficiency in optical and wireless networks, big data, cloud computing, and Internet of Things.

SYED ALI RAZA ZAIDI (Senior Member, IEEE) received the Ph.D. degree from the School of Electronic and Electrical Engineering, University of Leeds.

From 2011 to 2013, he was associated with the International University of Rabat working as a Research Associate. He was also a Visiting Research Scientist with Qatar Innovations and Mobility Centre from October 2013 to December 2013 working on QNRF-funded project QSON. From 2013 to 2015, he was associated with the SPCOM Research Group working on U.S. ARL-funded project in the area of network science. He is currently an Associate Professor with the University of Leeds in the broad area of communication and sensing for robotics and autonomous systems. He has published more than 90 papers in leading IEEE conferences and journals. He has been awarded COST IC0902, Royal Academy of Engineering, EPSRC, Horizon EU, and DAAD grants to promote his research outputs. His current research interests include ICT, applied mathematics, mobile computing, and embedded systems implementation. Specifically, his current research is geared toward: design and implementation of communication protocols to enable various applications (rehabilitation, healthcare, manufacturing, and surveillance) of future RAS, and design, implementation, and control of RAS for enabling future wireless networks (e.g., autonomous deployment and management and repair of future cellular networks). He was awarded the G. W. and F. W. Carter Prize for best thesis and best research paper. From 2014 to 2015, he was an Editor of the IEEE COMMUNICATION LETTERS and a Lead Guest Editor of *IET Signal Processing* special issue on Signal Processing for Large Scale 5G Wireless Networks. He is also an Editor of IET Access, Fronthaul, and Backhaul books. He is also serving as an Associate Technical Editor for *IEEE Communications Magazine*.